DOI: 10.1002/chem.200601588

A "Green Route" to Propene through Selective Hydrogen Oxidation

Jan Hendrik Blank,[a] Jurriaan Beckers,[a] Paul F. Collignon,[a] Frédéric Clerc,[b] and Gadi Rothenberg*[a]

Abstract: The pros and cons of oxidative dehydrogenation of propane are outlined and a new catalytic system based on metal-doped cerianite catalysts is introduced. These novel materials catalyze the selective combustion of hydrogen from a mixture of hydrogen, propane, and propene at 550 °C. This gives three key advantages: energy is supplied directly where needed, product separation is made easier, and the dehydrogenation equilibrium is shifted to the desired products. A set of eighteen doped cerianites was synthesized in parallel, characterized, and screened for activity, selectivity, and stability in a cyclic redox system. The best results were obtained with $Ce_{0.89}Cr_{0.02}Fe_{0.09}O_2$, $Ce_{0.98}Sn_{0.02}O_2$, and $Ce_{0.96}Cu_{0.02}Zn_{0.02}O_2$, which gave 98 %, 91 %, and 98 % selectivity, respectively. $Ce_{0.89}Cr_{0.02}Fe_{0.09}O_2$ also shows excellent stability in over 120 cycles (66 h on stream at 550 °C). Importantly, these doped cerias are monophasic crystalline materials. The dopants are incorporated as solid solutions throughout the fluorite lattice. This means that these catalysts are very stable (they do not sinter during reduction) as opposed to traditional supported metal oxides. The results show that both activity and selectivity towards hydrogen combustion can be tuned (increased or decreased) by selecting the appropriate dopant. Furthermore, the trends in selectivity differ from those measured on supported oxides of the same elements, which indicates that these novel materials indeed contain unique active sites. The factors governing selectivity towards hydrogen oxidation and the nature of the active site are discussed.

Keywords: cerium · green chemistry · heterogeneous catalysis · hydrogen combustion · solid solutions

Introduction

Propene is an important bulk chemical. It is used primarily for producing (poly)propene for a variety of applications, from pipes to yoghurt pots and margarine tubs.[1] The demand for high-purity propene is increasing rapidly.[2] In 2003, it was 56 million metric tons, and estimates for 2010 are as high as 80 million metric tons. The market growth is 5–6 % per annum for propene and ≈7 % per annum for (poly)propene.[3–5] Much of this demand originates in the Chinese industry sector. The record high crude oil prices have also sent international (poly)propene resin prices soaring, and producers are operating their plants at ≈90 % capacity.[6]

Over 95 % of the propene produced on an industrial scale is obtained through naphtha cracking, in which it is co-produced with ethene. More advantageous "on-purpose" production is achieved by metathesis, methanol to olefin, and catalytic dehydrogenation of propane.[4,7] The last process usually employs a platinum or chromium oxide catalyst on alumina, and produces only propene and hydrogen. Unfortunately, this dehydrogenation is an equilibrium that favors the products only at high temperature and low pressure (Scheme 1, top). Moreover, separating propene and hydrogen is not trivial.

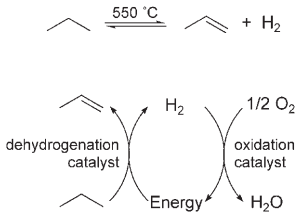

Scheme 1. Dehydrogenation equilibrium (top) and dehydrogenation combined with selective hydrogen combustion (bottom).

[a] J. H. Blank, J. Beckers, P. F. Collignon, Dr. G. Rothenberg
Van't Hoff Institute for Molecular Sciences
University of Amsterdam, Nieuwe Achtergracht 166
1018 WV Amsterdam (The Netherlands)
Fax: (+31) 20-525-5604
E-mail: gadi@science.uva.nl

[b] Dr. F. Clerc
Institut de Recherches sur la Catalyse-CNRS
2, Avenue Albert Einstein, 69626 Villeurbanne (France)

One way to solve these problems is by burning the hydrogen byproduct (Scheme 1, bottom). This generates energy and shifts the equilibrium to the desired products. Furthermore, it is easier to separate propene from water than from hydrogen. The ABB Lummus SMART process successfully applies this concept for dehydrogenation of ethyl benzene, albeit at lower temperatures.[8] This combination of dehydrogenation and selective hydrogen combustion can be carried out in either "co-fed mode" or "redox" mode (Scheme 2).[9–21] Most of the research on oxidative dehydrogenation (ODH) deals with the co-fed process. In this scenario, propane (or ethane) is mixed with a small amount of dioxygen and the mixture is flowed over the catalyst. This catalyst performs both the dehydrogenation and the hydrogen oxidation. The process runs until coke formation renders the catalyst ineffective, after which the catalyst is regenerated. Grasselli and co-workers reported >97% selectivity and good activity and stability for In_2O_3/ZrO_2 catalysts, and similar selectivity for silica-supported Sb_2O_4, WO_3, and Bi_2O_3.[9] Oxides of vanadium and molybdenum are also frequently used.[14,20,22,23] The main disadvantage of the co-fed approach is that mixing oxygen, propane, propene, and hydrogen at 550°C in the presence of a catalyst is dangerous, so most industries avoid it. Alternatively, in the redox mode, two catalysts are employed: a dehydrogenation catalyst, such as, platinum or chromium oxide on alumina, and a selective hydrogen combustion (SHC) catalyst. The SHC catalyst acts as an "oxygen reservoir", and is recharged with oxygen in every cycle before the reducing gases are fed through. This prevents the mixing of dioxygen with the reductive gases, and allows separate tuning of the dehydrogenation and SHC processes.

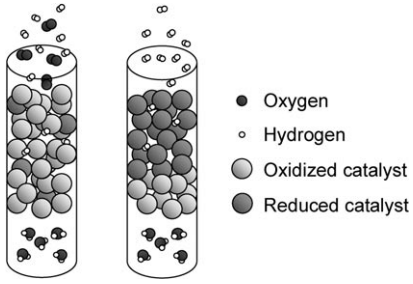

Scheme 2. General oxidation in co-fed (left) and redox mode (right). Note that the redox operation is a cyclic process, in which the bed is flushed with an inert gas between reduction and oxidation steps.

Grasselli and co-workers,[10,11] and we[24] showed that supported oxides of p-block metals can catalyze the selective oxidation of hydrogen in the presence of C_2 and C_3 hydrocarbons in redox mode. These catalysts give good selectivity (>99.8%), and the active-oxide loading can be as high as 30–50%. However, most of these metals melt below or around 500–700°C, and thus, sinter during the reduction step.[10] Here, we present a new type of SHC catalyst. In a preliminary communication, working with hydrogen/ethane/ethene mixtures, we demonstrated the "oxygen reservoir" by using a series of doped cerium oxides.[25] Ceria is known for its ability to store, release, and transport oxygen, and doping can be used to tune the $2\,CeO_2 \rightleftarrows Ce_2O_3 + O$ redox cycle.[26,27] Choosing the right dopant can increase the selectivity towards hydrogen oxidation.

In this paper, we apply the same approach for the first time to the hydrogen/propane/propene system. We describe the synthesis and characterization of a set of eighteen new doped cerium oxides, and discuss the results obtained from testing these in a specialized setup that allowed control over the redox cycle conditions. Most importantly, we discovered that $Ce_{0.89}Cr_{0.02}Fe_{0.09}O_2$ is an excellent catalyst for selective hydrogen oxidation, and showed that the catalysts' performance depends strongly on the dopants.

Results and Discussion

Catalyst preparation and characterization: The eighteen doped cerianites were prepared in parallel by co-melting the appropriate metal nitrate salts followed by calcination.[25] This method enabled the preparation of multiple samples on a 5–10 g scale (Figure 1, left). In a typical synthesis, the metal nitrates (or chlorides or ammonium metallates when nitrates were not available) were co-melted under vacuum, left to boil for four hours, and then calcined at 700°C, ground, and sieved (70–120 mesh). Table 1 details the catalysts' composition, surface area, and activity and selectivity for hydrogen combustion. We used 33 different elements as dopants, with the general catalyst formula $Ce_{1-x-y}M^1_xM^2_yO_2$. Each catalyst was characterized by using powder X-ray diffraction, to ensure it consisted of a uniform phase. Figure 1 shows two typical X-ray diffraction patterns obtained for monophasic (top right) and biphasic (bottom right) materials. In all cases, the X-ray diffraction patterns were compared with that of pure CeO_2. No broad peaks at around 15°, indicating the presence of amorphous phases, were observed.

The rationale behind choosing the dopant compositions and quantities was based on two assumptions. First, because it is possible that oxygen atoms and/or oxygen vacancies in the fluorite lattice are influenced by one or two neighboring dopant cations, it is unlikely that *three* different neighboring dopant cations will simultaneously influence the same site. Second, an upper limit of the total cation doping of 20 mol% was chosen because high amounts of dopant increase the chance of separate phases forming.[28,29] As for the selection of the dopant type, we covered a wide range of the periodic table, selecting elements from different groups and periods. Toxic elements and those that do not form uniform solid solutions with ceria were excluded.

In addition to catalysts **1**–**18**, we also tried preparing $Ce_{0.9}In_{0.1}O_2$ (**19**), $Ce_{0.88}Ni_{0.10}Sm_{0.02}O_2$ (**20**), $Ce_{0.87}Ag_{0.08}Sr_{0.05}O_2$ (**21**), $Ce_{0.9}Au_{0.1}O_2$ (**22**), $Ce_{0.84}Mo_{0.08}V_{0.08}O_2$ (**23**), $Ce_{0.9}Pb_{0.1}O_2$ (**24**), and $Ce_{0.9}Li_{0.1}O_2$ (**25**). However, all of these samples showed secondary phases that were identified as the dopant oxides or dopant metals (see, for example, Figure 1, bottom

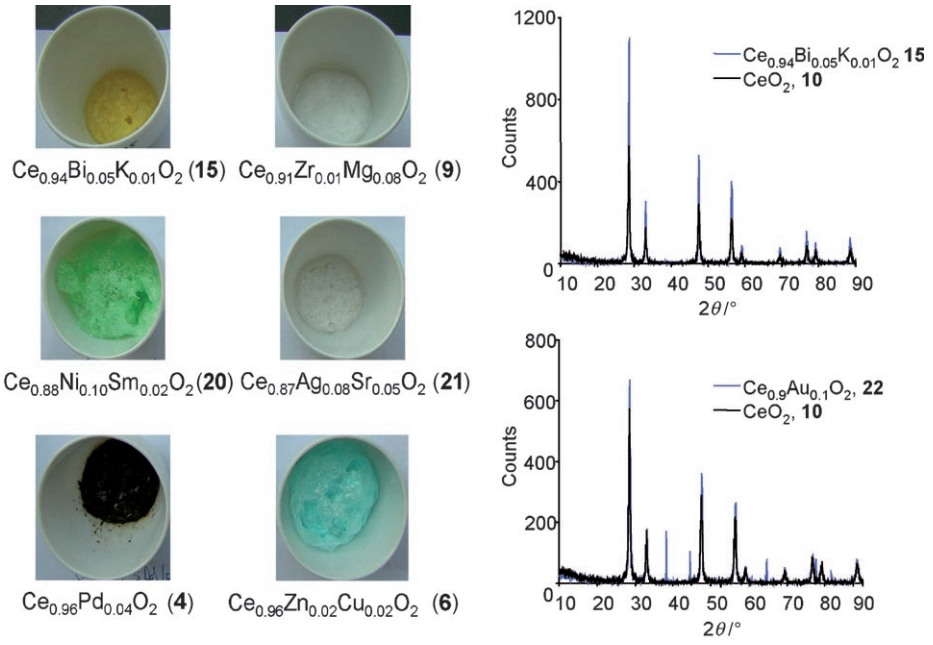

Figure 1. Left: Photo of doped-cerianite solid solutions, obtained by co-melting and boiling under vacuum. Right: X-ray diffraction patterns for catalysts **10**, **15**, and a catalyst (**22**) containing 10 mol% Au. Catalyst **15** is homogeneous. The extra peaks in the spectrum of catalyst **22** pertain to metallic gold.

Table 1. Composition, surface area (*s*), and catalytic activity of doped cerianites **1**–**18**.

Catalyst	Composition[a]	Dopant precursor(s)[b]	*s* [$m^2 g^{-1}$]	Activity[c] [$\mu mol(O\,atoms)\,m^{-2}$]	H_2 oxidation selectivity[c] [%]
1	$Ce_{0.87}Al_{0.08}Ta_{0.05}O_2$	$Al(NO_3)_3{\cdot}9H_2O$ $TaCl_5$	58	7	–
2	$Ce_{0.96}Ca_{0.02}Sr_{0.02}O_2$	$Ca(NO_3)_2{\cdot}4H_2O$ $Sr(NO_3)_2$	42	6	18
3	$Ce_{0.89}Cr_{0.02}Fe_{0.09}O_2$	$Cr(NO_3)_3{\cdot}9H_2O$ $Fe(NO_3)_3{\cdot}9H_2O$	28	24	98
4	$Ce_{0.96}Pd_{0.04}O_2$	$Pd(NO_3)_2{\cdot}2H_2O$	53	54	–
5	$Ce_{0.98}Sn_{0.02}O_2$	$SnCl_2{\cdot}2H_2O$	67	7	91
6	$Ce_{0.96}Zn_{0.02}Cu_{0.02}O_2$	$Zn(NO_3)_2{\cdot}6H_2O$ $Cu(NO_3)_2{\cdot}3H_2O$	44	11	98
7	$Ce_{0.89}Pt_{0.02}Mn_{0.09}O_2$	$PtCl_4$ $Mn(NO_3)_2{\cdot}4H_2O$	57	40	–
8	$Ce_{0.92}Ta_{0.05}Ti_{0.03}O_2$	$TaCl_5/TiCl_4$	46	8	–
9	$Ce_{0.91}Zr_{0.01}Mg_{0.08}O_2$	$ZrO(NO_3)_2{\cdot}xH_2O$ $Mg(NO_3)_2{\cdot}6H_2O$	26	10	40
10	CeO_2	–	51	6	35
11	$Ce_{0.90}Nd_{0.10}O_2$	$Nd(NO_3)_3{\cdot}6H_2O$	61	5	–
12	$Ce_{0.90}Yb_{0.08}Gd_{0.02}O_2$	$Yb(NO_3)_3{\cdot}5H_2O$ $Gd(NO_3)_3{\cdot}6H_2O$	24	15	40
13	$Ce_{0.93}Ru_{0.02}Sm_{0.05}O_2$	$RuCl_3$ $Sm(NO_3)_3{\cdot}6H_2O$	65	51	–
14	$Ce_{0.90}Y_{0.05}Sr_{0.05}O_2$	$Y(NO_3)_3{\cdot}5H_2O$ $Sr(NO_3)_2$	27	12	44
15	$Ce_{0.94}Bi_{0.05}K_{0.01}O_2$	$Bi(NO_3)_3{\cdot}5H_2O$ KNO_3	17	34	73
16	$Ce_{0.91}La_{0.09}O_2$	$La(NO_3)_3{\cdot}6H_2O$	49	8	–
17	$Ce_{0.9}W_{0.1}O_2$	$(NH_4)_{10}W_{12}O_{41}{\cdot}5H_2O$	25	12	–
18	$Ce_{0.96}Cr_{0.04}O_2$	$Cr(NO_3)_3{\cdot}9H_2O$	24	22	92

[a] Determined by using ICP. Ta and W could not be quantified by using ICP, and are calculated from the precursor relative amounts. [b] In all cases, $Ce(NO_3)_3{\cdot}6H_2O$ was used as the Ce precursor. [c] Activity and selectivity values at 550 °C, averaged over 14 cycles.

right). Of the 33 chosen dopants, 25 showed proper mixing of the dopant, thus yielding a monophasic solid solution. The biphasic samples were not tested further at this stage because we wanted to evaluate the catalytic properties of doped ceria. When all tests had been performed, we synthesized and tested three of our samples (**3**, **5**, and **15**) again to verify the reproducibility (**3b**, **5b**, and **15b**). X-ray diffraction characterization measurements on these samples showed a uniform single phase.

Oxygen consumption and exchange activity: In a typical reaction, a stream simulating the effluent from industrial propane dehydrogenation (7% $C_3H_8/C_3H_6/H_2$ (5:1:1 v/v) in N_2 at a total flow rate of 50 mL min^{-1}) was fed to the reactor containing doped cerianite (≈250 mg) at 550 °C. Following this ten-minute reduction step, the reactor was purged with N_2, followed by an oxidation step (1% v/v O_2 in N_2, 18 min) and a second purge step with N_2 to complete the cycle. The reaction was monitored by using continuous mass spectrometry (MS) and online gas chromatography (GC).

Our goal was to find a solid oxygen carrier that oxidizes hydrogen selectively in the presence of the propane and propene. In addition to this reaction, however, several side processes may occur. First, either or both of the hydrocarbons can combust to CO/CO_2 and water. Coking, leading to a carbon deposit on the catalyst and formation of gaseous hydrogen is also possible. In this process smaller hydrocarbon fragments such as methane, ethane, and ethene may also form. Finally, propene can hydrogenate, and propane can dehydrogenate. All of these processes were taken into account in the data analysis. We defined the activity as the total amount of oxygen uptake

during the reoxidation step (note that CO could not be quantified on the mass spectrum due to overlap with the N_2 signal). For example, pure cerium oxide **10** consumed 6 μmol of oxygen atoms per square meter of catalyst in every cycle. Activity is expressed per square meter of catalyst surface to account for the different surface areas of the materials (the typical surface area of these materials is approximately 40 $m^2 g^{-1}$). Duplicate samples were synthesized to assess the reproducibility of the activity determination. Values found were 24 and 34 μmol(O atoms) m^{-2} for samples **3** and **3b**, 7 and 9 μmol(O atoms) m^{-2} for **5** and **5b**, and 12 and 11 μmol(O atoms) m^{-2} for **17** and **17b**, respectively. The higher activity of **3b** relative to **3** originates from a higher propene conversion near the end of the reduction cycle. Possibly, propene conversion is more facile over reduced iron or chromium.

Figure 2 shows the activity per cycle for catalysts **1**–**3**, **5**, **6**, **8**–**12**, and **14**–**18**. Catalysts **4**, **7**, and **13**, which were doped with 4d and 5d metals from groups 8 and 10, are discussed

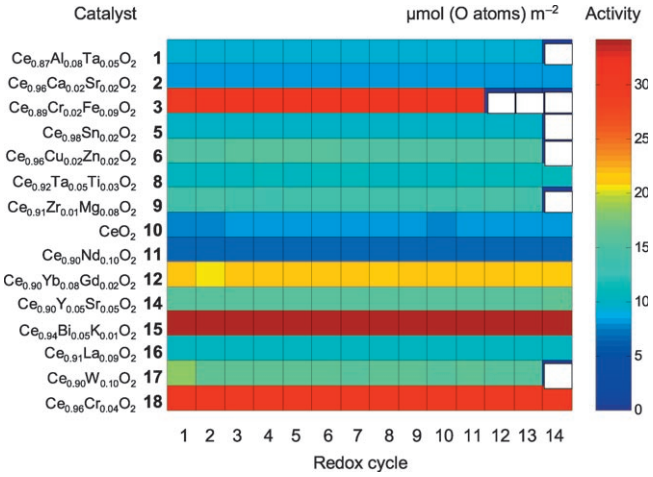

Figure 2. Total oxidation activity, shown as absolute amounts of available oxygen (μmol of O atoms per m^2 of catalyst) for fourteen consecutive cycles (white: not measured). Catalysts **4**, **7**, and **13** are omitted for clarity.

separately. These three catalysts show extremely high activity, but this is unfortunately only due to the total oxidation of all the reactants. The activity data is normalized for the surface area of each catalyst to allow a fair comparison. No trend was observed when activity was compared on a "per dopant atom" basis. This shows that the activity is related to the type of dopant and not merely to the amount of doping.

Relative to pure cerium oxide, most dopants promote more oxygen release from the lattice. This is not surprising, as doping creates lattice defects.[30,31] The most active catalyst, $Ce_{0.94}Bi_{0.05}K_{0.01}O_2$ (**15**), consumes 34 μmol m^{-2}, followed by **3**, **18**, and **12** (24, 22, and 15 μmol m^{-2}, respectively). Surprisingly, catalyst $Ce_{0.90}Nd_{0.10}O_2$ (**11**) is *less* active than pure cerium oxide (5 μmol m^{-2}). These results show the unique possibilities of tuning the cerianite activity by doping, through which it can be both increased and decreased.

Selectivity towards hydrogen oxidation: The selectivity to H_2 oxidation was calculated by using Equation (1):

$$\frac{H_2 \text{ conversion}}{\text{total conversion}} \times 100 \qquad (1)$$

The total conversion is the sum of the hydrogen, propane, and propene conversion. When determining the selectivity, one must take into account possible side reactions. For example, if a catalyst that facilitates C_3H_8 dehydrogenation also catalyses C_3H_6 oxidation, the net conversion of C_3H_6 would be around zero, with simultaneous H_2 formation and C_3H_8 conversion. The same outcome, however, could also result from a catalyst that leaves the C_3H_6 untouched and cracks C_3H_8, forming H_2 and coke. Because of this complexity, one cannot simply compare all of the catalysts in the same way. Instead, we divided the catalysts into three groups, based upon the extent of the side reactions described above. All the results pertain to the first GC measurement performed in each cycle. Subsequent measurements of most samples showed no more conversion, which indicated that the lattice oxygen was depleted.

For the first group we could only assign a qualitative level of selectivity. This group consisted of catalysts **4**, **7**, and **13**, which contain noble metals (Pd, Pt, and Ru, respectively). These catalysts showed such a high extent of side reactions (mainly total oxidation and coking), that no conclusion about the processes occurring at the catalyst surface could be drawn. However, due to the high extent of side reactions, the selectivity of this type of catalyst was low.

The second group consisted of catalysts **1**, **8**, **11**, **16**, and **17**, which contained the elements Al, Ta, Ti, La, Nd, and W. The catalysts within this group showed comparable results: a small amount of hydrogen is formed (5–10%), propane conversion is zero or low, and 5–20% of the propene is converted. The presence of CO_2 and water in the reactor effluent and the net production of hydrogen indicated that propene combustion and coking occurred simultaneously. If the hydrogen had been formed from propane dehydrogenation, the propane conversion would not have been zero. The results show that these catalysts are not selective because a selective catalyst would have a much higher rate of hydrogen combustion compared with hydrocarbon combustion.

The third group of catalysts were selective enough to enable quantification. They displayed high hydrogen conversion and low or no hydrocarbon conversion. These were catalysts **2**, **3**, **5**, **6**, **9**, **10**, **12**, **14**, **15**, and **18**. We used undoped CeO_2 (catalyst **10**, 35% selectivity) as a reference point. The most selective catalysts for H_2 oxidation were **3**, **5**, **6**, and **18** (98, 91, 98, and 92% selectivity, respectively). These catalysts contained the elements Cu, Cr, Fe, Sn, and Zn. Catalyst **15** showed a selectivity of 73% and **9**, **12**, and **14**, all containing lanthanides and alkaline-earth metals, showed selectivities of 40–44%, only slightly higher than the undoped CeO_2. Catalyst **2** showed a preference for oxidizing hydrocarbons, with only 18% selectivity to H_2 oxidation. To assess reproducibility, the duplicate samples **3b**, **5b**, and **15b**

were synthesized with the same precursor composition as **3**, **5**, and **15**. The measured selectivities were 98 and 95% for **3** and **3b**, 91 and 77% for **5** and **5b**, and 73 and 76% for **15** and **15b**, respectively.

The nature of the active site: A selective catalyst will oxidize hydrogen, but not hydrocarbons. The results show that doping the ceria can both enhance and reduce selectivity towards hydrogen combustion. The amount of hydrogen oxidation, coking of hydrocarbons, and oxidation of hydrocarbons varies widely over the set. It is important to realize that the dopants can influence the catalytic properties of the crystal in two ways. Firstly, the dopant atoms themselves can function as active sites. In this case, differences in activity can be correlated to the different electronic properties of the dopant. Secondly, the nature of the oxygen, such as its binding energy in the lattice, may be influenced by the presence of the dopant. This could be due to the electronic properties of the dopant or to the difference in size relative to ceria, creating stress in the lattice that may facilitate oxygen release. The catalysts in group one (**4**, **7**, and **13**) showed that both processes do indeed occur. CO_2 and/or CO form in the initial part of the reduction step, which indicates interaction of the hydrocarbons with the lattice oxygen. However, where the other catalysts show zero or low activity in the remainder of the reduction step, catalysts **4**, **7**, and **13** continue to convert the hydrocarbons under the formation of large amounts of hydrogen, and, in the case of catalyst **13** ($Ce_{0.93}Ru_{0.02}Sm_{0.05}O_2$), in the absence of CO_2 and CO. In a separate experiment, we reduced catalyst **4** ($Ce_{0.96}Pd_{0.04}O_2$) in a H_2/N_2 (5% v/v) stream for one hour, removing all the available oxygen from the lattice. After this we fed in the propane/propene mixture. Indeed, this generated large amounts of H_2 and fractions of hydrocarbon fragments (C_2H_4, C_2H_6, and CH_4), but neither CO_2 nor CO was observed, even at full hydrocarbon conversion. This means that the (reduced) dopant acts as an active site. In time, the activity does drop, presumably because of coking on the surface. Note that a catalyst that is selective in its oxidized state may become less selective when reduced. The Cr/Fe catalysts (**3**/**3b**) display this behavior, in which 2 to 6% of the propene feed was coked in the latter part of the reduction cycle.

In theory, a partially reduced dopant could also be a selective active site, if it would promote dissociative hydrogen adsorption without affecting the propane or propene. This hydrogen could be more active towards the remainder of the surface oxygen or diffuse into the lattice and react there. We have no indication that this occurs because the catalysts of group three (the most selective ones) showed little or no activity in the latter part of the reduction step. However, they did oxidize part of the gas feed in the initial stage. Because no gaseous oxygen was present, it follows that the differences in selectivity for these catalysts are related to the nature of the lattice oxygen (binding energy and Lewis basicity[32]). If the dopant were to decrease the binding energy of this oxygen, we would expect a decrease in selectivity. On the other hand, if the binding energy were to increase, selectivity can be increased owing to a lower affinity towards the hydrocarbons.[33] The selectivity results of group three show that even low dopant amounts (e.g., 2% dopant for **5**, or 4% dopant for **6**) can result in a highly selective catalyst. The coordination number of oxygen in the fluorite lattice is four (at the surface it will be lower). Thus, one needs at least 25% dopant to ensure that every oxygen atom is adjacent to a dopant atom. The fact that catalysts with a much lower amount of doping can still be selective indicates either that the dopants have a long-range influence on the oxygen atoms, or that the surface is enriched with dopant atoms. Surface enrichment has been observed for these types of catalysts.[34–36] With this in mind, one wonders whether the doped fluorite lattice is accountable for the selectivity, or just offers a stable support for the dopant oxides. However, in the latter case, one would expect the same trends in selectivity as seen for the supported oxides,[9,24] which is not the case.[25] Combined with the X-ray diffraction results, we conclude that these materials indeed contain unique active sites that facilitate the selective hydrogen combustion.

With the exception of catalyst **5** (2% Sn), the catalysts with selectivity higher than 90% (**3**, **5**, **6**, **18**) contained dopants positioned close together in the periodic table (Cr, Fe, Cu, Zn). This prompted us to search for a correlation between selectivity and atomic properties. We used the Pauling electronegativity scale, as it reflects the electronic properties of both the dopants and the lattice oxygen.[37] We see that the electronegativity is roughly correlated with the selectivity. The catalysts in group one have electronegativities in the range of 2.2–2.28 (please note that groups one, two, and three refer to our grouping of the catalysts according to their selectivity and not to the groups of the periodic table). In group two, the electronegativity ranges from 1.10–1.54 (in **17**, W is an exception with 2.36). The elements of group three that display a low selectivity have electronegativities from 0.95 to 1.33, and the highly selective elements have values between 1.65 and 1.91. However, this is a very simplified model of a complex system.

Surprisingly, we observed a clear difference in selectivity between ethane/ethene and propane/propene mixtures. In our previous work,[25] tungsten-doped ceria gave 97% selectivity for hydrogen combustion from an ethane/ethene mixture ($C_2H_6/C_2H_4/H_2$/He (20:20:5:55% v/v), 600°C). Here, the selectivity for the same catalyst (**17**) was only 52%. The difference is not merely based on the more facile combustion of C_3 relative to C_2 hydrocarbons because the selectivity of the W catalyst was lower when using C_3 hydrocarbons, but that of the tin-doped and bismuth-doped catalysts **5** and **15** was not. To exclude any irreproducibility owing to catalyst preparation, we also tested the exact same batch of $Ce_{0.90}W_{0.10}O_2$ that was used in the previous research with C_2 hydrocarbons. This gave results identical to those of the new batch. The catalyst does not interact with propane, but the values for propene and hydrogen conversion are equal, which leads to the drop in selectivity. Zhao and Gorte[38]

also observed that doping ceria may affect the relative rates for C_1–C_4 hydrocarbon oxidation, in their case by using gaseous oxygen. For undoped ceria, the rates of propane and *n*-butane oxidation increased sharply relative to those of methane and ethane. However, a samarium-doped catalyst showed comparable rates for all four hydrocarbons. The differences were ascribed to different reaction mechanisms.

Activity versus selectivity: When comparing the catalyst groups one to three, one sees a trend between the activity and selectivity. The unselective catalysts of group one show a much higher activity than the more selective catalysts of group three. Figure 3 shows the activity versus selectivity for

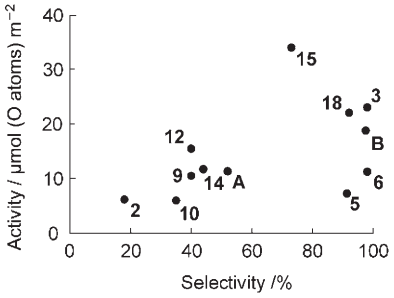

Figure 3. Activity versus selectivity for the catalysts of group three. Points **A** and **B** denote data for the $Ce_{0.90}W_{0.10}O_2$ catalyst with propane/propene and ethane/ethene mixtures, respectively.

group three (catalysts **2**, **3**, **5**, **6**, **9**, **10**, **12**, **14**, **15**, and **18**). Points **A** and **B** denote data for $Ce_{0.90}W_{0.10}O_2$ in hydrogen combustion from propane/propene and ethane/ethene mixtures, respectively (see above). The figure shows that for group three, high activity is not linked to low selectivity. The promising candidates (**3** and **18**) show both high selectivity and activity and both catalysts contain chromium. The activity of the selective catalysts **5** and **6** is lower, which may be related to the lower amount of doping. Note that there is no general trend between the activity and the level of doping, because catalysts **9**, **12**, **14**, and **3**, **15**, and **18** all contain about 10 mol% of dopant, but differ significantly in activity.

Catalyst stability: One key advantage of doped cerias over supported metal oxides is their inherent stability. As the dopant forms part of the fluorite lattice there is little chance of sintering.[24,25] Indeed, except for **6**, which gave a metallic residue at the reactor outlet, the catalysts showed no signs of degradation over 10–15 redox cycles (typically 6–8 h at 550 °C). To further test this stability, we ran a separate experiment by using catalyst **3**, the most promising candidate in terms of activity and selectivity. This catalyst was kept at 550 °C for 66 h (123 redox cycles), while the activity and selectivity were monitored. As Figure 4 shows, the decrease in activity over 100 cycles was only 9.6%. The selectivity towards H_2 oxidation shows large deviations during the first half of the experiment (80–100%),[39] after which it stabilizes at ≈98%. Comparing the BET surface area of a fresh

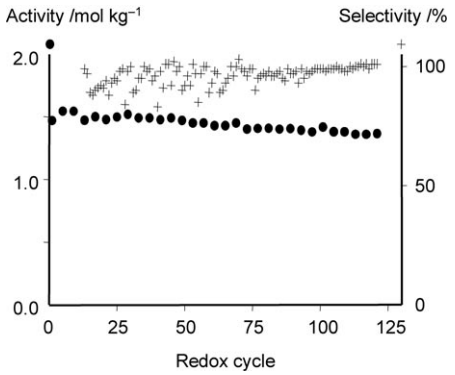

Figure 4. Activity (●) and selectivity (+) of catalyst **3** ($Ce_{0.89}Cr_{0.02}Fe_{0.09}O_2$) during 66 h on stream at 550 °C (123 redox cycles).

sample of **3** with that of the same sample after 134 redox cycles showed a reduction from 20 to 13 $m^2 g^{-1}$. This decrease in the surface area is attributed to a partial breakdown of the pore structure.

Conclusion

Co-melting of nitrate salts is a simple and easy protocol for making doped cerianites. Monophasic crystalline materials form in many cases, provided that the dopant concentration is not too high. This method is unsuitable, however, for doping with In, Ni, Ag, Au, V, Mo, Pb, and Li. These dopants form separate phases. The doped cerianites can be used as selective hydrogen oxidation catalysts, and display a range of oxidation activity and selectivity that strongly depend on the type and amount of dopant. Contrary to supported oxides, these single-phase lattices are stable during multiple redox cycles. The best catalyst in this set, $Ce_{0.89}Cr_{0.02}Fe_{0.09}O_2$ (**3**), showed high activity (24 μmol(O atoms) m^{-2}) and high selectivity towards H_2 oxidation (98%) for over 123 redox cycles (66 h at 550 °C). Conversely, doping with 4d and 5d metals from groups 8 and 10 is not useful in this case, because the resulting catalysts catalyze cracking and (de)hydrogenation as well as oxidation. Burning the hydrogen byproduct may seem wasteful, but one should bear in mind that the energy is supplied exactly where it is needed. The hydrogen combustion heats the bed that is cooled by the dehydrogenation reaction. The ease of separating propene from water and the positive shift in the dehydrogenation equilibrium are additional advantages. In general, metal-doped cerianites are good candidates for catalyzing selective hydrogen combustion in the presence of C_3 hydrocarbons. The facile synthesis and strong property–composition relationship makes these materials ideal for "fine-tuning" by using combinatorial methods such as genetic algorithms.[40] Such an optimization will be the subject of future research in our laboratory.

Experimental Section

Materials and instrumentation: GC analysis was performed by using an Interscience CompactGC instrument, which separated H_2, CO, CH_4, O_2, and N_2 on a 5 Å molecular sieve (Molsieve) column (Ar carrier gas), and C_2 and C_3 hydrocarbons, water, and CO_2 on a Porabond Q column (He carrier gas). MS analysis was performed by using a Pfeiffer QMS 200 mass spectrometer (m/z range: 0–200). Ar was used as the tracer in the oxidative gas feed for marking the start of each cycle. Inductive coupled plasma (ICP) measurements were performed on a Perkin Optima 3000XL ICP instrument. Samples were prepared by using a Perkin–Elmer microwave sample preparation system. Powder X-ray diffraction was performed by using a Philips PW-series X-ray diffractometer with a Cu-tube radiation source ($\lambda = 1.54$ Å), a vertical axis goniometer, and a proportional detector. The 2θ detection measurement range was 10–90° with a 0.025° step size and a 5 s dwell time. Catalyst surface areas were measured by N_2 adsorption at 77 K by using a Sorptomatic 99 (CE Instruments) apparatus and calculated by using the BET equation. Chemicals were purchased from commercial sources. All gases were purchased from Praxair (>99.5% purity). He, O_2, Ar, and N_2 streams were further purified over BTS columns and/or molecular sieves.

Procedure for catalyst synthesis: Doped cerianites were prepared by sequential co-melting, drying, and calcining of mixed-metal nitrates ($Ce(NO_3)_3{\cdot}6H_2O$ in the case of ceria) as published previously.[25] Where nitrate precursors were not available, chlorides or ammonium metallates were used. This was the case for Ru, Pt, Sn, Ti, and Ta (chloride salts were used, in the case of Sn the chloride hydrate salt was used) and for V and W (NH_4VO_3 and $(NH_4)_{10}W_{12}O_{41}{\cdot}5H_2O$ were used). **CAUTION!** Although none of our samples gave off the brownish vapor associated with nitrous gases, all preparations should be carried out in a well-ventilated fume hood.

General method using $Ce_{0.92}Ta_{0.05}Ti_{0.03}O_2$ (10) as an example: $Ce(NO_3)_3{\cdot}6H_2O$ (3.739 g), $TiCl_4$ (0.091 g), and $TaCl_5$ (0.172 g) were put in an open porcelain vessel. The vessel was placed in a vacuum oven preheated to 110 °C. After the salts were allowed to melt for 5 min, the pressure was lowered carefully, making sure that no vigorous boiling occurred. Samples were left for about 15 min at the pressure at which they were just starting to boil. After this, the pressure was lowered to <10 mbar and kept for 4 h, to obtain a brightly colored solid. This solid was then calcined at 700 °C in static air (ramp rate: 300 °C h^{-1}, hold time: 5 h), pulverized, ground, and sieved (70–120 mesh, 125–212 μm).

ICP analysis: Prior to the analysis, the metals were brought into solution by heating the sample (approximately 50 mg) in aqua regia (6 mL) to 170–200 °C by using a microwave oven. These temperatures were held for 25 min, during which the pressure rose to 40–55 bar. After the samples had been cooled, the volume was brought to 100 mL with demineralized water. This sample was diluted 100 times before analysis. Cerium recovery from a pure ceria sample by using this method was 98.3% ($n = 6$). W, K, and Ta could not be determined by using this method. An alternative method involving gentle heating in a mixture of concentrated HF (5 mL) and 2 M H_2SO_4 (2 mL) for 2 h did not work either. Therefore the concentration of these elements was calculated from the amount of precursors weighed.

Selective hydrogen combustion experiments: Activity, selectivity, and stability were determined by using an automated cyclic redox reactor system built in-house. The sample was charged to quartz wool in a tubular quartz reactor (4 mm i.d.), which was placed in a water-cooled oven. In each experiment, doped cerianite catalyst (≈250 mg) was placed in the reactor and heated to 550 °C with a ramp rate of 1200 °C h^{-1}. The redox cycling began with an 18 min oxidation step, by using a feed of 1% v/v O_2 and 1% v/v Ar (tracer) in N_2 at 50 mL min^{-1}. This was followed by a 3 min purge with pure N_2 (50 mL min^{-1}) and a 10 min reduction step by using a feed of 5% v/v propane, 1% v/v propene, and 1% v/v H_2 in N_2 as the balance gas (total flow rate: 50 mL min^{-1}). After another 3 min purging step, the next oxidation cycle began. Conversion and selectivity were measured by using GC and MS for 14 consecutive cycles. The setup maintained a constant pressure during the switching between oxidative, reductive, and purge-gas feeds, preventing over- or underestimation of the analyte concentration. This was done by adjusting the backpressure of the vent to the same value as the reactor back pressure, and switching the gases between the reactor and this pressurized vent. The product selectivity was determined by using GC. Four consecutive GC measurements were performed for each reductive cycle, the first one starting at $t = 50$ s. This time was a trade off between the time window in which the catalyst was still active (i.e., the time it took for the available lattice oxygen to be depleted), and the time needed for flushing out the N_2 from the previous purge step. With 250 mg catalyst, the activity window was smaller than the flush-out time, leading to an overestimation of the conversion. Therefore, conversion was corrected by using measurements on a blank reactor, filled with an amount of quartz wool yielding the same backpressure as a typical sample (1.10–1.24 bar). The catalytic activity (measured as oxygen uptake) was determined by continuous mass spectrometry. When the catalyst was active, no oxygen signals appeared at the beginning of the cycle to time t. This time t, together with the flow rate and the concentration of oxygen in the feed was used to calculate the total oxygen uptake of the catalyst sample.

Acknowledgements

We thank A. J. van Wijk and L. Hoitinga for performing the ICP measurements, A. C. Moleman for help with the X-ray diffraction measurements, and M. C. Mittelmeijer-Hazeleger for fruitful discussions and the BET surface-area measurements. This research was financed by the Netherlands Organisation for Scientific Research—Advanced Catalytic Technologies for Sustainability (NWO-ACTS) ASPECT program

[1] E. Burridge, *Chem. Bus.* **2006**, *1*, 45.
[2] J. Plotkin, E. Glatzer, *Eur. Chem. News* **2005**, *82*, 20–22.
[3] G. Ondrey, *Chem. Eng.* **2004**, *111*, 20–24.
[4] G. Parkinson, *Chem. Eng. Prog.* **2004**, *100*, 8–11.
[5] N. Alperowicz, *Chem. Week* **2005**, *167*, 26–31.
[6] P. H. Sim, *Chem. Week* **2004**, *166*, 29.
[7] A. L. Waddans, *Chemicals from Petroleum*, 4th ed., John Murray, London, **1978**.
[8] F. M. Dautzenberg, P. J. Angevine, *Catal. Today* **2004**, *93–95*, 3–16.
[9] R. K. Grasselli, D. L. Stern, J. G. Tsikoyiannis, *Appl. Catal. A* **1999**, *189*, 1–8.
[10] R. K. Grasselli, D. L. Stern, J. G. Tsikoyiannis, *Appl. Catal. A* **1999**, *189*, 9–14.
[11] J. G. Tsikoyiannis, D. L. Stern, R. K. Grasselli, *J. Catal.* **1999**, *184*, 77–86.
[12] L. Låte, J. I. Rundereim, E. A. Blekkan, *Appl. Catal. A* **2004**, *262*, 53–61.
[13] L. Låte, W. Thelin, E. A. Blekkan, *Appl. Catal. A* **2004**, *262*, 63–68.
[14] L. Jalowiecki-Duhamel, A. Ponchel, C. Lamonier, A. D'Huysser, Y. Barbaux, *Langmuir* **2001**, *17*, 1511–1517.
[15] S. Bergh, P. J. Cong, B. Ehnebuske, S. H. Guan, A. Hagemeyer, H. Lin, Y. M. Liu, C. G. Lugmair, H. W. Turner, A. F. Volpe, W. H. Weinberg, L. Woo, J. Zysk, *Top Catal.* **2003**, *23*, 65–79.
[16] Y. M. Liu, P. J. Cong, R. D. Doolen, S. H. Guan, V. Markov, L. Woo, S. Zeyss, U. Dingerdissen, *Appl. Catal. A* **2003**, *254*, 59–66.
[17] O. V. Buyevskaya, A. Bruckner, E. V. Kondratenko, D. Wolf, M. Baerns, *Catal. Today* **2001**, *67*, 369–378.
[18] O. V. Buyevskaya, D. Wolf, M. Baerns, *Catal. Today* **2000**, *62*, 91–99.
[19] E. V. Kondratenko, O. V. Buyevskaya, M. Baerns, *Top Catal* **2001**, *15*, 175–180.
[20] R. Grabowski, *Catal. Rev.-Sci. Eng.* **2006**, *48*, 199–268.
[21] M. A. Banares, *Catal. Today* **1999**, *51*, 319–348.
[22] E. Heracleous, A. A. Lemonidou, J. A. Lercher, *Appl. Catal. A* **2004**, *264*, 73–80.
[23] T. Blasco, J. M. L. Nieto, *Appl. Catal. A* **1997**, *157*, 117–142.
[24] L. M. Van der Zande, E. A. de Graaf, G. Rothenberg, *Adv. Synth. Catal.* **2002**, *344*, 884–889.

[25] G. Rothenberg, E. A. de Graaf, A. Bliek, *Angew. Chem.* **2003**, *115*, 3488–3490; *Angew. Chem. Int. Ed.* **2003**, *42*, 3366–3368.
[26] N. V. Skorodumova, S. I. Simak, B. I. Lundqvist, I. A. Abrikosov, B. Johansson, *Phys. Rev. Lett.* **2002**, *89*, 166601.
[27] E. Aneggi, M. Boaro, C. de Leitenburg, G. Dolcetti, A. Trovarelli, *J. Alloys Compd.* **2006**, *408*, 1096–1102.
[28] A. E. C. Palmqvist, M. Wirde, U. Gelius, M. Muhammed, *Nanostruct. Mater.* **1999**, *11*, 995–1007.
[29] M. Mogensen, N. M. Sammes, G. A. Tompsett, *Solid State Ionics* **2000**, *129*, 63–94.
[30] P. J. Gellings, H. J. M. Bouwmeester, *Catal. Today* **2000**, *58*, 1–53.
[31] D. A. Andersson, S. I. Simak, N. V. Skorodumova, I. A. Abrikosov, B. Johansson, *Proc. Natl. Acad. Sci. USA* **2006**, *103*, 3518–3521.
[32] R. Burch, D. J. Crittle, M. J. Hayes, *Catal. Today* **1999**, *47*, 229–234.
[33] R. K. Grasselli, *Top. Catal.* **2002**, *21*, 79–88.
[34] G. Rothenberg, E. A. de Graaf, J. Beckers, A. Bliek, *Catal. Org. React.* **2005**, *104*, 201–210.
[35] P. J. Scanlon, R. A. M. Bink, F. P. F. van Berkel, G. M. Christie, L. J. van Ijzendoorn, H. H. Brongersma, R. G. Van Welzenis, *Solid State Ionics* **1998**, *112*, 123–130.
[36] T. X. T. Sayle, S. C. Parker, C. R. A. Catlow, *J. Phys. Chem.* **1994**, *98*, 13625–13630.
[37] L. Pauling, *The Nature of the Chemical Bond*, 3rd ed., Cornell University Press, Ithaca, N.Y., **1960**.
[38] S. Zhao, R. J. Gorte, *Appl. Catal. A* **2004**, *277*, 129–136.
[39] The initial deviation in selectivity was attributed to an unstable propene mass-flow controller. After fixing this problem, a repeat with catalyst **3b** gave stable selectivity values over 125 cycles (95% selectivity with a standard deviation of 2.2).
[40] F. Clerc, M. Lengliz, D. Farrusseng, C. Mirodatos, S. R. M. Pereira, R. Rakotomalala, *Rev. Sci. Instrum.* **2005**, *76*, 062208.

Received: November 7, 2006
Published online: April 12, 2007

